*Journal of Alloys and Compounds, 203* (1994) 251–257
*JALCOM 884*



# Magnetic studies on alkali metal uranates(V) $MUO_3$ with the perovskite structure

Yukio Hinatsu
*Department of Chemistry, Japan Atomic Energy Research Institute, Tokai-mura, Ibaraki 319-11 (Japan)*

(Received July 5, 1993)

**Abstract**

The magnetic properties of alkali metal uranates(V) $MUO_3$ (M, alkali metal) with the perovskite structure have been studied. In this study $RbUO_3$ (cubic perovskite structure) was prepared and its magnetic susceptibility was measured from 4.2 K to room temperature. It was found that a magnetic anomaly (magnetic transition) occurred at about 27 K. As a result of the $U^{5+}$ ion in the paramagnetic state, the electron paramagnetic resonance spectrum was not observed even at 4.2 K. The magnetic susceptibility results and the optical absorption spectrum were analysed on the basis of an octahedral crystal field model. The magnetic transition temperatures and crystal field parameters determined for $MUO_3$ (M ≡ Li, Na, K, Rb) are compared and discussed.

## 1. Introduction

The magnetic and optical properties of actinides are characterized by the behaviour of the 5f electrons. For the 5f compounds the crystal field, spin–orbit coupling and electron–electron repulsion interactions are of comparable magnitude, which makes the analysis of the experimental results complicated. However, in the case of actinide ions with the [Rn]$5f^1$ electronic configuration, *e.g.* the $U^{5+}$ ion, the situation is simplified considerably, because there are no electronic repulsion interactions. Therefore the theoretical treatment of such ions becomes much easier and we can obtain a deeper understanding of the behaviour of 5f electrons in solids.

Among the many uranium complex oxides, the alkali metal uranates $MUO_3$ (M ≡ Li, Na, K, Rb) attract our attention. X-ray structure analysis indicates that these uranates have a (distorted) perovskite-type structure, *i.e.* the uranium ion is (nearly) octahedrally coordinated by six oxygen ions. This high coordination symmetry around the $U^{5+}$ ion in addition to the $f^1$ configuration enables us to analyse the experimental results easily. In this paper we have studied the magnetic properties of $RbUO_3$, which has a cubic perovskite structure (space group $O_h^1$–$Pm3m$) [1]. Although the magnetic and optical properties of $RbUO_3$ provide suitable information for a detailed comparison with theoretical calculations, surprisingly few measurements have been carried out.

Kemmler-Sack *et al.* [2] measured the magnetic susceptibility of $RbUO_3$ from 90 to 453 K and reported that it could be represented by $\chi = 0.050/T + 450 \times 10^{-6}$ e.m.u. $mol^{-1}$. Later Kemmler-Sack [3] measured the reflectance spectrum of $RbUO_3$ and analysed it on the basis of the $5f^1$ configuration for the $U^{5+}$ ion in an octahedral crystal field. Miyake *et al.* [4] extended the temperature range of the magnetic susceptibility measurements of $RbUO_3$ down to 2.0 K and reported that a spike was found at 32–33 K in the magnetic susceptibility *vs.* temperature curve. They also reported that a broad electron paramagnetic resonance (EPR) spectrum was obtained at room temperature and 77 K and that the $g$ value was larger than two (2.43–2.48). Concerning the magnetic susceptibility anomaly at about 32 K and the EPR spectrum of $RbUO_3$ measured by Miyake *et al.* [4], Edelstein and Goffart [5] raise a question in their review article and consider that both results are incorrect.

In a previous paper [6] we reported that $KUO_3$ shows a magnetic transition at about 16 K and that its transition temperature decreases with increasing magnetic field. Because $RbUO_3$ is isostructural with $KUO_3$, similar magnetic interaction is expected to be found. In order to study the magnetic properties of the 5f electron in an octahedral crystal field, we have prepared $RbUO_3$ and carried out magnetic susceptibility measurements on it in the temperature range between 4.2 K and room temperature. EPR measurements have been carried out on $RbUO_3$ diluted with isostructural $BaUO_3$ (temperature-independent paramagnetic). The crystal field parameters for $RbUO_3$ are determined from the analysis of its optical spectrum reported earlier [3]. The results of the magnetic susceptibility and EPR


*SSDI* 0925-8388(93)00884-2

measurements on $RbUO_3$ together with those for $LiUO_3$, $NaUO_3$ and $KUO_3$ will be discussed on the basis of the octahedral crystal field model.

## 2. Experimental details

### 2.1. Preparation

$RbUO_3$ was prepared by the following reactions [7]:

$$U_3O_8 + 3Rb_2CO_3 \xrightarrow{\text{in air}} 3Rb_2UO_4 + 3CO_2 \quad (1)$$

$$Rb_2UO_4 + UO_2 \xrightarrow{\text{in vacuo}} 2RbUO_3 \quad (2)$$

$Rb_2UO_4$ was prepared by firing intimately ground mixtures of $U_3O_8$ and $Rb_2CO_3$ in air at 850 °C for 1 day. After cooling, the same grinding and firing were repeated. $RbUO_3$ was prepared by heating mixtures of $UO_2$ and excess $Rb_2UO_4$ in an evacuated quartz tube at 650 °C for 10 h. To avoid the reaction of $Rb_2UO_4$ and $UO_2$ with quartz, the mixtures were wrapped in molybdenum foil. After cooling to room temperature, the sample was crushed into a powder, pressed into pellets and reacted under the same conditions.

For EPR measurements $RbUO_3$ was diluted with isostructural $BaUO_3$ by heating mixtures of $RbUO_3$ and $BaUO_3$ in an evacuated quartz tube at 650 °C for 2 days. The ratios of $RbUO_3$ in $BaUO_3$ were 2 and 5 mol%.

### 2.2. Analysis

#### 2.2.1. X-Ray diffraction analysis

An X-ray diffraction study was performed with Cu K$\alpha$ radiation on a Philips PW 1390 diffractometer equipped with a curved graphite monochromator. The lattice parameter of the sample was determined by a least-squares method applied to the diffraction lines.

#### 2.2.2. Determination of oxygen amount

The oxygen non-stoichiometry in the sample was checked by the back-titration method [8, 9]. A weighed sample was dissolved in excess cerium(IV) sulphate solution which had been standardized in advance with stoichiometric $UO_2$. Then the excess cerium(IV) was titrated against a standard iron(II) ammonium sulphate solution with ferroin indicator. The oxygen amount was determined for a predetermined Rb/U ratio.

### 2.3. Magnetic susceptibility measurement

The magnetic susceptibility was measured with a Faraday-type torsion balance in the temperature range between 4.2 K and room temperature. The apparatus was calibrated with a manganese Tutton salt ($\chi_g = 10\,980 \times 10^{-6}/(T+0.7)$) standard. The temperature of the sample was measured by a "normal" Ag *vs.* Au–0.07at.%Fe thermocouple (4.2–40 K) [10] or an Au–Co *vs.* Cu thermocouple (from 10 K to room temperature). To examine the field dependence, the magnetic susceptibility was measured at field strengths of 2800, 4700, 6900, 9000 and 10 600 G. Details of the experimental procedure have been given elsewhere [11].

### 2.4. Electron paramagnetic resonance measurement

The EPR measurements were carried out both at room temperature and at 4.2 K for the specimen sealed in a quartz tube. The measurements were made using a Jeol RE-2X spectrometer operating at X-band frequency (about 9.10 GHz) with 100 kHz field modulation. The magnetic field was swept from 100 to 13 000 G. Before measuring the specimen, a blank was recorded to eliminate the possibility of interference by the background resonance of the cavity and/or sample tube.

## 3. Results and discussion

The X-ray diffraction analysis shows that the $RbUO_3$ prepared in this study is cubic and that the lattice parameter is $a = 4.326$ Å. The chemical analysis of the oxygen concentration gives the formula $RbUO_{2.996}$. In view of the error limits for this analysis, this result indicates that the specimen is oxygen stoichiometric.

Figure 1 shows the magnetic susceptibility *vs.* temperature curve for $RbUO_3$. We have found that the susceptibility shows a maximum at about 28 K. This magnetic anomaly is similar to that found by Miyake *et al.* [4], but the temperature is lower than that reported by those authors. A similar behaviour has been found for the magnetic susceptibility of $KUO_3$, which has the same cubic perovskite structure as $RbUO_3$ [4, 6]. Fur-

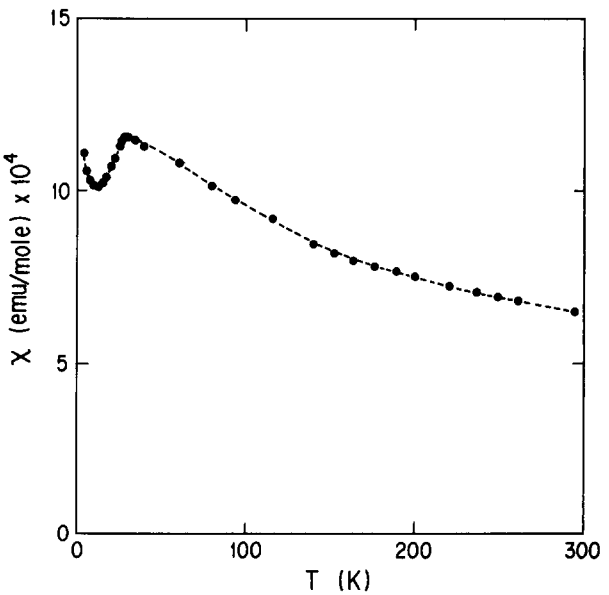


Fig. 1. Magnetic susceptibility *vs.* temperature curve for $RbUO_3$.

thermore, $NaUO_3$, which has a $GdFeO_3$-type crystal structure [12], also shows a similar anomaly at 31.1 K in the magnetic susceptibility [13]; this magnetic anomaly has been supported by the finding of a heat capacity anomaly [14]. These magnetic anomalies have been attributed to the transition to long-range ordering [6, 13, 15]. We consider that the magnetic anomaly found at about 27 K is also due to the long-range magnetic ordering between uranium ions. To examine the similarity of the field dependence of the magnetic susceptibility of $RbUO_3$ to that of $KUO_3$, we have measured the magnetic susceptibility of $RbUO_3$ at various magnetic fields. No field dependence of the magnetic susceptibility is found apart from a weak dependence at 4.2 K and the magnetic transition temperature does not change with magnetic field. This result is different from that for $KUO_3$, where the susceptibility below 25 K depends on the magnetic field and the magnetic transition temperature decreases with increasing magnetic field [6].

Lewis *et al.* [16] reported that no EPR signal from the $U^{5+}$ ion could be detected in concentrated alkali metal uranates. This is probably because of the strong magnetic interaction between uranium ions (rapid spin–spin interaction) in the concentrated compounds. To decrease the effect of this magnetic interaction between uranium ions, we have diluted the $RbUO_3$ with $BaUO_3$ for the EPR measurements. Because oxygen-stoichiometric $BaUO_3$ shows temperature-independent paramagnetism over a wide temperature range [17], $RbUO_3$ diluted with $BaUO_3$ is considered to show a magnetic property of the $U^{5+}$ ion perturbed by the octahedral crystal field in addition to the temperature-independent paramagnetism of the $U^{4+}$ ion. A broad EPR spectrum was observed even at room temperature and the $g$ value was about 2.3. This result is similar to that reported for concentrated $RbUO_3$ by Miyake *et al.* [4]. As will be discussed later, we have considered that this EPR spectrum with large $g$ value ($g > 2$) is not ascribable to the paramagnetic property of the $U^{5+}$ ion perturbed by the octahedral crystal field, but that it may be related to the magnetic interaction between uranium ions as is found at low temperatures.

In $RbUO_3$ the $U^{5+}$ ion is octahedrally coordinated by six oxygen ions. This high coordination symmetry in addition to the one-electron configuration ([Rn]$5f^1$) enables us to analyse the magnetic properties theoretically. It is convenient to use as the basis set the energy levels of the $f^1$ ion in a strong crystal field. Figure 2 shows the effects of perturbing the $f^1$ orbital energy levels successively by an octahedral crystal field and spin–orbit coupling. In the crystal field with octahedral symmetry the sevenfold-degenerate energy state of the f orbitals is split into $\Gamma_2$, $\Gamma_5$ and $\Gamma_4$ states,

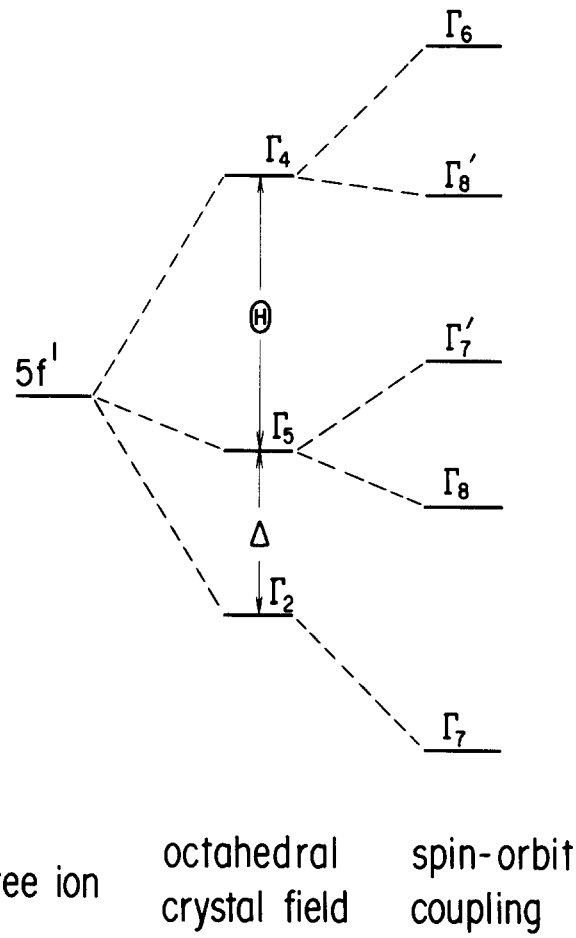


Fig. 2. Splitting of $f^1$ orbital perturbed by octahedral crystal field and spin–orbit coupling.

where $\Delta$ and $\Theta$ are parameters representing the intensity of the crystal field. When spin–orbit coupling is taken into account, the $\Gamma_2$ orbital state is transformed into $\Gamma_7$, whereas the $\Gamma_5$ and $\Gamma_4$ states are split into $\Gamma_7^*$ and $\Gamma_8$, and $\Gamma_6$ and $\Gamma_8^*$ respectively. The ground state Kramers doublet is the $\Gamma_7$ state and is coupled to the excited $\Gamma_7^*$ state arising from the $\Gamma_5$ orbital by spin–orbit coupling. The energy matrices for the $\Gamma_7$, $\Gamma_8$ and $\Gamma_6$ states are

$$\Gamma_7: \begin{vmatrix} 0 & (3k)^{1/2}\zeta \\ (3k)^{1/2}\zeta & \Delta - \frac{1}{2}k\zeta \end{vmatrix}$$

$$\Gamma_8: \begin{vmatrix} \Delta + \frac{1}{4}k\zeta & \frac{3}{4}(5kk')^{1/2}\zeta \\ \frac{3}{4}(5kk')^{1/2}\zeta & \Delta + \Theta - \frac{3}{4}k'\zeta \end{vmatrix} \qquad (3)$$

$$\Gamma_6: \left|\Delta + \Theta + \tfrac{3}{2}k'\zeta\right|$$

Here $\zeta$ is the spin–orbit coupling constant and $k$ and $k'$ are the orbital reduction factors for an electron in the $\Gamma_5$ and $\Gamma_4$ orbital states respectively [18, 19]. Dia-

gonalization of the energy matrix produces the ground state $\Gamma_7$ and the excited state $\Gamma'_7$. The corresponding wavefunctions are written as

$$|\Gamma_7\rangle = \cos\theta|^2F_{5/2}, \Gamma_7\rangle - \sin\theta|^2F_{5/2}, \Gamma_7^*\rangle$$
$$|\Gamma'_7\rangle = \sin\theta|^2F_{5/2}, \Gamma_7\rangle + \cos\theta|^2F_{5/2}, \Gamma_7^*\rangle \quad (4)$$

where $\theta$ is a parameter describing the admixture of the $\Gamma_7$ levels in the ground state via the relation

$$\tan(2\theta) = \frac{2(3k)^{1/2}\zeta}{\Delta - \frac{1}{2}k\zeta} \quad (5)$$

Similarly, diagonalization of the $\Gamma_8$ matrix produces the two levels $\Gamma_8$ and $\Gamma'_8$ with the corresponding wavefunctions

$$|\Gamma_8\rangle = \cos\phi|^2F_{5/2}, \Gamma_8\rangle - \sin\phi|^2F_{7/2}, \Gamma_8^*\rangle$$
$$|\Gamma'_8\rangle = \sin\phi|^2F_{5/2}, \Gamma_8\rangle + \cos\phi|^2F_{7/2}, \Gamma_8^*\rangle \quad (6)$$

where $\phi$ is a parameter describing the admixture of the $\Gamma_8$ levels in the excited state via

$$\tan(2\phi) = \frac{\frac{3}{2}(5kk')^{1/2}\zeta}{\Theta - [(k+3k')/4]\zeta} \quad (7)$$

The energies for the $\Gamma_7$, $\Gamma_8$, $\Gamma'_7$, $\Gamma'_8$ and $\Gamma_6$ levels are

$$E(\Gamma_7) = \Delta - \tfrac{1}{2}[k + 2(3k)^{1/2}\cot\theta]\zeta$$
$$E(\Gamma_8) = \Delta + \Theta - \tfrac{3}{4}[k' + (5kk')^{1/2}\cot\phi]\zeta$$
$$E(\Gamma'_7) = (3k)^{1/2}\zeta\cot\theta \quad (8)$$
$$E(\Gamma'_8) = \Delta + \tfrac{1}{4}[k + 3(5kk')^{1/2}\cot\phi]\zeta$$
$$E(\Gamma_6) = \Delta + \Theta + \tfrac{3}{2}k'\zeta$$

The $g$ value for the ground $\Gamma_7$ doublet is calculated as

$$g = 2\langle\Gamma_7|L + 2S|\Gamma_7\rangle$$
$$= 2\cos^2\theta - 4(k/3)^{1/2}\sin(2\theta) - \tfrac{2}{3}(1-k)\sin^2\theta \quad (9)$$

This equation indicates that the $g$ value for an f electron perturbed by the octahedral crystal field should be between $-1.43$ and 2.00 even if the covalency effect $k$ is included [20]. Figure 3 shows the variation in $g$ value for $k = 1$ and 0.95 as a function of the relative strength of the crystal field and spin–orbit interaction, $\Delta/(7/2\zeta)$. Therefore the EPR spectrum with large $g$ value ($g > 2$) measured in this experiment is not ascribable to the paramagnetic behaviour of the $U^{5+}$ ion perturbed by the octahedral crystal field. We have considered that it may be related to the magnetic interaction between $U^{5+}$ ions. Similar arguments have been made for the large $g$ value observed in other $U^{5+}$ compounds [4, 21, 22].

The determination of the crystal field parameters $\Delta$ and $\Theta$, the orbital reduction factors $k$ and $k'$ and the spin–orbit coupling constant $\zeta$ in eqns. (8) requires the

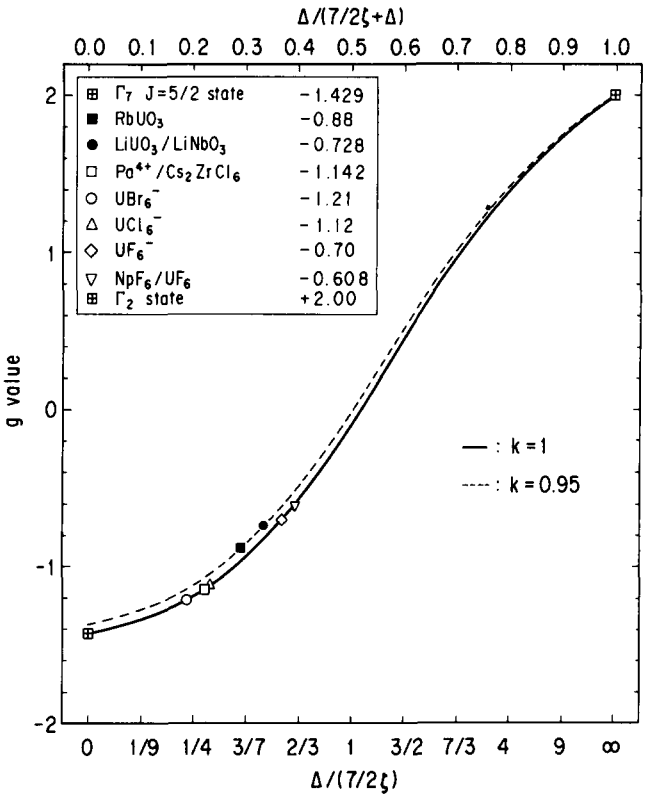


Fig. 3. Plot of $g$ value *vs.* relative strength of crystal field and spin–orbit interaction, $\Delta/(7/2\zeta)$, for a number of $f^1$ compounds in octahedral symmetry.

TABLE 1. Crystal field parameters and orbital reduction factors

| | Experiment | Calculation |
|---|---|---|
| $\Gamma_7 \rightarrow \Gamma_8$ ($cm^{-1}$) | 4274 | 4177 |
| $\Gamma_7 \rightarrow \Gamma'_7$ ($cm^{-1}$) | 6757 | 6758 |
| $\Gamma_7 \rightarrow \Gamma'_8$ ($cm^{-1}$) | 9615 | 10499 |
| $\Gamma_7 \rightarrow \Gamma_6$ ($cm^{-1}$) | 12195 | 12195 |
| $g$ value | $\lvert g\rvert = 0.88$[a] | $g = -0.88$ |
| $\zeta$ ($cm^{-1}$) | | 1917 |
| $\Delta$ ($cm^{-1}$) | | 2855 |
| $\Theta$ ($cm^{-1}$) | | 4776 |
| $k$ | | 0.95 |
| $k'$ | | 0.75 |

[a]This value was determined from the temperature-dependent part of the magnetic susceptibility (see text).

assignment of the optical transitions. The optical spectrum for $RbUO_3$ measured by Kemmler-Sack [3] shows no splitting of the $\Gamma_7 \rightarrow \Gamma_8$ and $\Gamma_7 \rightarrow \Gamma'_8$ transitions, *i.e.* the central $U^{5+}$ ion is in a crystal field with octahedral symmetry. The transition energies are listed in Table 1. To obtain reliable crystal field parameters and orbital reduction factors, we need the information on the ground state $\Gamma_7$. Although the EPR measurements do not give the $g$ value for the ground state $\Gamma_7$, this value can be determined from the temperature-dependent part of

the magnetic susceptibility, which will be described in the following.

The magnetic susceptibility of the molecule is given by

$$\chi = \frac{N \sum_{n,m} [(E^{(1)}_{n,m})^2/kT - 2E^{(2)}_{n,m}] \exp(-E^0_{n,m}/kT)}{\sum_{n,m} \exp(-E^0_{n,m}/kT)} \quad (10)$$

where $N$ is the Avogadro number, $E^0_{n,m}$ is the zero-field energy, $E^{(1)}_{n,m}$ and $E^{(2)}_{n,m}$ are the first- and second-order Zeeman terms respectively, $n$ and $m$ are quantum numbers and $k$ is the Boltzmann constant. If the separation of levels within the ground state is much smaller and the energy of the next excited state is much larger than $kT$, the susceptibility is expressed in the form [23]

$$\chi = \frac{Ng^2\beta^2}{4kT} + \chi_{TIP} \quad (11)$$

where

$$\chi_{TIP} = 2N\beta^2 \sum_i \frac{|\langle \Gamma_i|L + 2S|\Gamma_7\rangle|^2}{E(\Gamma_i) - E(\Gamma_7)} \quad (12)$$

The $g$ value in eqn. (11) is the same $g$ value obtained from EPR measurements on the ground crystal field state (eqn. (9)), *i.e.* the $g$ value can be determined from this temperature-dependent part of the susceptibility. From the extrapolation of $1/T$ to zero for the measured magnetic susceptibility ($\chi_{exp}$) *vs.* reciprocal temperature ($1/T$) curve, we may obtain the temperature-independent paramagnetic susceptibility $\chi_{TIP} = 430 \times 10^{-6}$ e.m.u. mol$^{-1}$. The resulting temperature-dependent susceptibility ($\chi(T) = \chi_{exp} - \chi_{TIP}$) follows the equation $\chi(T) = 0.0728/(T + 31.9)$ except at very low temperatures. From this temperature-dependent part of the susceptibility (using eqn. (11)) the $g$ value for the ground state of the $U^{5+}$ ion in $RbUO_3$ is calculated to be 0.88. This $g$ value is quite reasonable for an $f^1$ electron perturbed by the octahedral crystal field and comparable $g$ values are found in many $5f^1$ compounds [24–27].

Now we can determine the crystal field parameters and orbital reduction factors by fitting the calculated (eqns. (8)) transition energies to those determined experimentally (Table 1) and by fitting the calculated (eqn. (9)) $g$ value to that obtained from the magnetic susceptibility measurements ($|g| = 0.88$). However, not all the calculated transition energies can be fitted to the experimental results. We have considered that the transition $\Gamma_7 \rightarrow \Gamma'_8$ is the least reliable one because it is known to be broad and sometimes split. The calculated transition energies and the crystal field parameters and orbital reduction factors determined here are listed in Table 1. The spin–orbit coupling constant is 1917 cm$^{-1}$, which is a reasonable value for the $U^{5+}$ ion in solids [28–31].

Next the magnetic susceptibility of $RbUO_3$ in the paramagnetic temperature region will be evaluated. Since we have already obtained the wavefunctions for the ground doublets and excited states (eqns. (4) and (6)), the magnetic susceptibility of $RbUO_3$ is easily calculated from eqn. (11) as

$$\chi = 0.0728/T + 214 \times 10^{-6} \quad (13)$$

A discrepancy between the calculated and experimental results is found in the temperature-independent part of the susceptibility. The value of $\chi_{TIP}$ obtained experimentally is larger than that calculated. This result suggests that some of the uranium ions are in the tetravalent state. The electronic configuration of the $U^{4+}$ ion is $[Rn]5f^2$. When a $5f^2$ ion is octahedrally coordinated by six anions, its susceptibility is known to show temperature-independent paramagnetism over a wide temperature range [32], *e.g.* as found in $BaUO_3$ [17].

In Fig. 4 we have plotted the magnetic transition temperature as a function of the nearest uranium–uranium distance for some uranium(V) complex oxides in which the $U^{5+}$ ion is in an octahedral or distorted octahedral crystal field. For $Ba_2MnUO_6$ the manganese ion also orders ferrimagnetically below 55 K [33] and therefore the distance on the abscissa of Fig. 4 is the nearest uranium–manganese distance. For comparison we have also included data for $BaPrO_3$, $BaTbO_3$, $SrTbO_3$ and $UO_2$ in the same figure [34–36]. $BaPrO_3$, $BaTbO_3$ and $SrTbO_3$ have a $GdFeO_3$-type crystal structure and the $Pr^{4+}$ ($4f^1$) and $Tb^{4+}$ ($4f^7$) ions

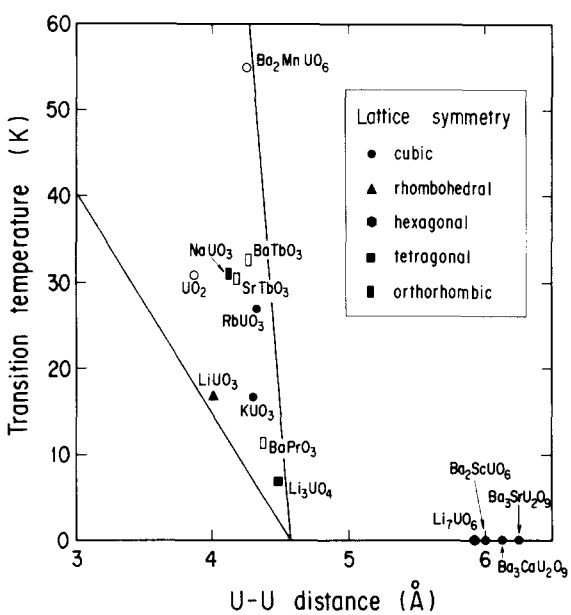


Fig. 4. Magnetic transition temperature *vs.* nearest uranium–uranium distance for a number of uranium complex oxides.

TABLE 2. Spin–orbit coupling constant and crystal field parameters

| | $LiUO_3$ | $NaUO_3$ | $KUO_3$ | $RbUO_3$ |
|---|---|---|---|---|
| $\zeta$ ($cm^{-1}$) | 1938 | 1954 | 1896 | 1917 |
| $\Delta$ ($cm^{-1}$) | 3543 | 3606 | 3335 | 2855 |
| $\Theta$ ($cm^{-1}$) | 6145 | 4857 | 4683 | 4776 |
| $k$ | 0.95 | 0.95 | 0.95 | 0.95 |
| $k'$ | 0.55 | 0.80 | 0.80 | 0.75 |
| $g$ | −0.728 | −0.72 | −0.76 | −0.88 |
| $T_{N,C}$ (K) | 16.9[a] | 31 | 16.8 | 27 |
| Crystal structure | Rhombohedral $LiNbO_3$ | Orthorhombic $GdFeO_3$ | Cubic perovskite | Cubic perovskite |
| $U^{5+}$–$U^{5+}$ (Å) | 4.004 | 4.125 | 4.294 | 4.326 |
| $U^{5+}$–$O^{2-}$ (Å) | 2.03 | 2.09 | 2.147 | 2.163 |

[a]This transition temperature is the one at which a large field dependence of the magnetic susceptibility is found.

are in a distorted octahedral crystal field. This figure indicates that the critical uranium–uranium distance for the magnetic exchange interaction is about 4.6 Å and that the transition temperature is independent of the crystal structure. It is quite reasonable that no magnetic exchange interaction is found in the uranium complex oxides with ordered perovskite structure, $Ba_2MUO_6$ (M≡Sc, Y) and $Ba_3MU_2O_9$ (M≡Ca, Sr) [33, 37], because the uranium–uranium distances are larger than the critical distance. It is also clear that the larger the uranium–uranium distance, the weaker is the magnetic interaction. Both $KUO_3$ and $RbUO_3$ have the same cubic perovskite structure and the lattice parameter (and therefore the nearest uranium–uranium distance) of $RbUO_3$ is larger than that of $KUO_3$. Therefore a lower transition temperature is expected for $RbUO_3$ than for $KUO_3$. The experimental results, however, show the opposite (Fig. 4). This result indicates that since this magnetic exchange interaction is not a direct uranium–uranium interaction but a super-exchange type of interaction via oxygen ions, a small difference in the uranium–uranium distance does not affect the magnetic interaction.

In Table 2 we have listed the crystal field parameters for $MUO_3$ (M≡Li, Na, K, Rb) with the perovskite structure. The parameters for $NaUO_3$ have been determined here by analysing both the magnetic susceptibility data reported by Kanellakopulos *et al.* [15] and the optical absorption spectrum data reported by Kemmler-Sack [3]. The spin–orbit coupling parameters are comparable with one another and are close to the value obtained from linear interpolation of the $\zeta$ values between the $Pa^{4+}$ and $Np^{6+}$ compounds, 1950 $cm^{-1}$ [38]. Among these $MUO_3$ compounds, the nearest U–O distance is the smallest for $LiUO_3$ and the largest for $RbUO_3$. Therefore the crystal field strength is the largest for $LiUO_3$ and the smallest for $RbUO_3$. Table 2 shows that the crystal field splitting ($\Delta + \Theta$) is the largest for $LiUO_3$ and the smallest for $RbUO_3$, as expected. In these $MUO_3$ perovskites the EPR spectrum of $U^{5+}$ has been measured only for $LiUO_3$ doped in isostructural $LiNbO_3$ and the $g$ value is −0.728 [16]. For other $MUO_3$ compounds we have determined the $g$ values by analysis of their optical spectra and magnetic susceptibilities. In the analysis we have considered the covalency effect $k$. Some of these $g$ values are plotted in the $g$ value *vs.* $\Delta/(7/2\zeta)$ curve of Fig. 3. These negative $g$ values lie between the values for $Pa^{4+}/Cs_2ZrCl_6$ (−1.142) (weak crystal field) [39] and $NpF_6/UF_6$ (−0.608) (strong crystal field) [24] and are comparable with the value for $UF_6^-$ (−0.70) [25, 26] but smaller than the values for $UCl_6^-$ (−1.12) and $UBr_6^-$ (−1.21) [27, 40, 41]. The $g$ value becomes increasingly negative from $LiUO_3$ to $RbUO_3$ (see also Table 2). This result means that the effect of the crystal field decreases from $LiUO_3$ to $RbUO_3$ (see the abscissa of Fig. 3), which corresponds to the crystal structural data (U–O distances in Table 2).

## References


1 W. Rüdorff, S. Kemmler-Sack and H. Leutner, *Angew. Chem., 74* (1962) 429.
2 S. Kemmler-Sack, E. Stumpp, W. Rüdorff and H. Erfurth, *Z. Anorg. Allg. Chem., 354* (1967) 287.
3 S. Kemmler-Sack, *Z. Anorg. Allg. Chem., 363* (1968) 295.
4 C. Miyake, K. Fuji and S. Imoto, *Chem. Phys. Lett., 61* (1979) 124.
5 N.M. Edelstein and J. Goffart, in J.J. Katz, G.T. Seaborg and L.R. Morss (eds.), *The Chemistry of the Actinide Elements,* Chapman and Hall, London/New York, 2nd edn., 1986, Chap. 18.
6 Y. Hinatsu, *J. Solid State Chem.,* in press.
7 S. Kemmler-Sack and W. Rüdorff, 354 (1967) 255.
8 S.R. Dharwadkar and M.S. Chandrasekharaiah, *Anal. Chim. Acta, 45* (1969) 545.
9 T. Fujino and T. Yamashita, *Fresenius' Z. Anal. Chem., 314* (1983) 156.
10 L.L. Sparks and R.L. Powell, *J. Res. NBS A, 76* (1972) 263.

11 Y. Hinatsu and T. Fujino, *J. Solid State Chem., 60* (1985) 195.
12 S.F. Bartram and R.E. Fryxell, *J. Inorg. Nucl. Chem., 32* (1970) 3701.
13 C. Miyake, K. Fuji and S. Imoto, *Chem. Phys. Lett., 46* (1977) 349.
14 W.G. Lyon, D.W. Osborne, H.E. Flotow and H.R. Hoekstra, *J. Chem. Thermodyn., 9* (1977) 201.
15 B. Kanellakopulos, E. Henrich, C. Keller, F. Baumgärtner, E. König and V.P. Desai, *Chem. Phys., 53* (1980) 197.
16 W.B. Lewis, H.G. Hecht and M.P. Eastman, *Inorg. Chem., 12* (1973) 1634.
17 Y. Hinatsu, *J. Solid State Chem., 102* (1993) 566.
18 J.C. Eisenstein and M.H.L. Pryce, *Proc. R. Soc. A, 255* (1960) 181.
19 H.G. Hecht, W.B. Lewis and M.P. Eastman, *Adv. Chem. Phys., 21* (1971) 351.
20 Y. Hinatsu, T. Fujino and N. Edelstein, *J. Solid State Chem., 99* (1992) 182.
21 C. Miyake, H. Takeuchi, H. Ohya-Nishiguchi and S. Imoto, *Phys. Status Solidi A, 74* (1982) 173.
22 Y. Hinatsu and T. Fujino, *Chem. Phys. Lett., 172* (1990) 131.
23 J.H. Van Vleck, *The Theory of Electronic and Magnetic Susceptibilities,* Oxford University Press, London, 1932.
24 C.A. Hutchison Jr. and B. Weinstock, *J. Chem. Phys., 32* (1960) 56.
25 P. Rigny and P. Plurien, *J. Phys. Chem. Solids, 28* (1967) 2589.
26 M. Dryfford, P. Rigny and P. Plurien, *Phys. Lett. A, 27* (1968) 620.
27 J. Selbin and H.J. Sherrill, *Inorg. Chem., 13* (1974) 1235.
28 D.G. Karraker, *Inorg. Chem., 3* (1964) 1618.
29 M.J. Reisfeld and G.A. Crosby, *Inorg. Chem., 4* (1965) 65.
30 N. Edelstein, D. Brown and B. Whittaker, *Inorg. Chem., 13* (1974) 563.
31 B. Kanellakopulos, *Gmelin Handbook of Inorganic Chemistry, Uranium,* Suppl. Vol. A6, Springer, New York/Berlin, 1983.
32 C.A. Hutchison Jr. and G.A. Candela, *J. Chem. Phys., 27* (1960) 707.
33 Y. Hinatsu, *J. Solid State Chem., 105* (1993) 100.
34 Y. Hinatsu, *J. Solid State Chem., 102* (1993) 362.
35 Y. Hinatsu, *J. Solid State Chem., 100* (1992) 136.
36 B.C. Frazer, G. Shirane, D.E. Cox and C.E. Olsen, *Phys. Rev., 140* (1965) A1448.
37 Y. Hinatsu, *J. Solid State Chem.,* in press.
38 J. Selbin and J.D. Ortego, *Chem. Rev., 69* (1969) 657.
39 J.D. Axe, H.J. Stapleton and C.D. Jeffries, *Phys. Rev., 121* (1961) 1630.
40 J. Selbin, J.D. Ortego and G. Gritzner, *Inorg. Chem., 7* (1968) 976.
41 J. Selbin, C. Ballhausen and D.G. Durrett, *Inorg. Chem., 11* (1972) 510.